

## FEM-Simulation of Single and Multi Layered Induction Heating Systems

Dr. A.K.M. AL-Shaikhli\*, Dr. Hanan A.R. Akkar\*  
& Dr.Mohammed Moanes Ezzaldeen Ali\*

Received on:4/1/2009

Accepted on:7/5/2009

### Abstract

Induction heating system has a number of inherent benefits compared to traditional heating systems. Many analytical and numerical approaches have been applied to solve the problem of induction heating; efforts are made to introduce new development in computational approaches and utilization of newly developed specialized software packages to improve the methods of analysis and design of induction heating systems. This paper includes the description of the steps used for developing a general and comprehensive program, which works under ANSYS 11.0SP1 package environment. This program can be applied to analyze a wide range of induction heating applications according to finite element method. Analysis approach is extended to deal with induction heating systems with magnetic material workpieces by introducing the multiregion method. Results of analysis the induction heating systems, by using ANSYS package, include all the electromagnetic and thermal quantities related to the induction heating process. To approve the simulation, used in this work, the results were compared with published practical measurements, a good agreement was achieved.

**Keywords:** Induction heating, finite element method, ANSYS, Multilayer

تمثيل منظومات التسخين الحثي احاديه و متعدده الطبقات باستخدام طريقه العنصر المحدد

### الخلاصه

تمتلك منظومات التسخين الحثي عده ميزات مقارنة بمنظومات التسخين التقليديه. هذه الميزات جعلت التسخين الحثي يشكل الحصة الرئيسييه من سوق معدات التسخين و الصهر. عدد كبير من الطرق التحليليه و العديديه استخدمت لتحليل و تصميم منظومات التسخين الحثي و الجهود مستمره لتطبيق اي تطور في البرامجيات و الطرق الحساييه لتطوير طرق التحليل و التصميم هذه. تتضمن هذه الورقه وصف لخطوات اعداد برنامج متكامل و عام يعمل ضمن بيئه ANSYS 11.0SP1، حيث يمكن استخدام هذا البرنامج بسهولة لتحليل تشكيله كبيره من تطبيقات التسخين الحثي اعتمادا على طريقه العنصر المحدد. تم توسيع طريقه التحليل لتكون قادره على التعامل مع منظومات التسخين ذوات قطع شغل مغناطيسييه و ذلك باستعمال مبدأ المناطق المتعدده. نتائج التحليل، المستخدم في هذه الورقه، تشمل كل الكميات الالكترومغناطيسييه و الحراريه المتعلقة بعملية التسخين الحثي. للتحقق من صلاحيه و دقة طريقه التحليل التي استخدمت في هذا البحث فقد تمت مقارنة النتائج مع قياسات عمليه منشوره، حيث كان التطابق بينهما جيد.

### 1-Introduction

The basic electromagnetic phenomena of induction heating are

quite simple. An alternating voltage applied to an induction coil (e.g. solenoid coil) will result in an

alternating current in the coil circuit. An alternating coil current will produce, in its surrounding, a time-variable magnetic field. This magnetic field induces eddy currents in the workpiece located inside the coil, these induced currents have the same frequency as the coil current but their direction is opposite to the coil current. These currents produce heat by the Joule effect ( $I^2R$ ).

The highest efficiencies, of induction heaters, are obtained when the electrical resistivity of the coil conductors is low compared to that of the workpiece, and minimum dimension of the workpiece, normal to the magnetic flux is large compared to skin depth. As the size of the workpiece decreases the efficiency is reduced. In single layer induction heating practice, use is then made of medium or high frequency power source to achieve the high efficiencies [1].

The efficiency can also be improved if a multi-layered coil is used instead of the conventional, single layer winding. The efficiency improvement is a consequence of reduced losses in the induction coil which results from its large effective cross-section. In single layer coil, the effective cross-section is limited by the skin depth in the coil conductors; whereas the conductor current of the multi layered coil, is uniformly distributed over the whole radial depth of the winding. The particular advantage of the multi layer technique is that the range of application of induction heating at mains frequency can be increased [2-4].

## 2- Analysis of Induction Heating Systems

Although the usage of multilayer induction heating systems

began later than the use of conventional single layer induction heating system by many decades, however it could be noted that the methods used to analyze the induction heating

problem are, almost, the same for single or multi layer coil, where it could be considered in analytical point of view that single layer is the special case of the general (multilayer) case. The Finite Element Method (FEM) could be considered to be the fastest growing technique in the area of electromagnetic applications where many FEM-based professional packages (such as ANSYS, FLUX2D, FLUX3D, etc.) are available to simulate various induction heating systems.

Induction heating process is a complex combination of electromagnetic, heat transfer, and metallurgical phenomena. These are tightly interrelated because the physical properties of heat-treated materials depend strongly on magnetic field intensity and temperature as well as chemical composition [1, 5]. This study concentrates on mathematical modeling of the electromagnetic field and thermal processes that occur during induction heating.

## 3- Mathematical Modeling of the Electromagnetic Field

The technique of calculating electromagnetic field depends on the ability to solve Maxwell's equations. For general time-varying electromagnetic fields, Maxwell's equations in differential form can be written as [6,7]:

$$\nabla \times H = J + \frac{\partial D}{\partial t} \quad \dots\dots (1)$$

$$\nabla \times E = -\frac{\partial B}{\partial t} \quad \dots\dots (2)$$

$$\nabla \cdot B = 0 \quad \dots\dots (3)$$

$$\nabla \cdot D = r^{charge} \quad \dots\dots (4)$$

Where E is the electric field intensity, D is the electric flux density, H is the magnetic field intensity, B is the magnetic flux density, J is conduction current density, and  $\rho^{charge}$  is electric volume charge density.

More equations are required because the number of equations is less than the number of unknowns. These equations are the following relations between the field quantities:

$$D = eE = \epsilon_0 \epsilon_r E \quad \dots\dots (5)$$

$$B = mH = \mu_0 \mu_r H \quad \dots\dots (6)$$

$$J = sE \quad \dots\dots (7)$$

Where the parameters  $\epsilon$ ,  $\mu$ , and  $\sigma$  denote, respectively, permittivity, magnetic permeability, and electrical conductivity of the material. For the most particular applications of the induction heating of metals, where the frequency of currents is less than 10MHz, the induced conduction current density J is much greater than the displacement current density  $\partial D / \partial t$ , so the equation (1) can be rewritten as:

$$\nabla \times H = sE \quad \dots\dots (8)$$

The magnetic flux density can be expressed in terms of magnetic vector potential A as:

$$B = \nabla \times A \quad \dots\dots (9)$$

And then from equations (2) and (9), it follows that:

$$\nabla \times E = -\nabla \times \frac{\partial A}{\partial t} \quad \dots\dots (10)$$

Therefore, after integration, one can obtain:

$$E = -\frac{\partial A}{\partial t} - \nabla \phi \quad \dots\dots (11)$$

Where  $\phi$  is the electric scalar potential and equation (7) can be written as:

$$J = -s \frac{\partial A}{\partial t} + J_s \quad \dots\dots (12)$$

Where  $J_s = -s \nabla^2 A$  is the source (excitation) current density in the induction coil.

Neglecting the hysteresis, it can be shown that [6, 8]:

$$\nabla \times \frac{1}{m} \nabla \times A + s \frac{\partial A}{\partial t} = J_s \quad \dots\dots (13)$$

For the great majority of induction heating applications, a heat effect, due to hysteresis losses, does not typically exceed 7% compared to the heat effect due to eddy current losses. Therefore, an assumption of neglecting the hysteresis is valid [5].

Equation (13) can be rewritten as follows according to the regions of the induction heating system [8]:

For workpiece:

$$\nabla \times \frac{1}{m} \nabla \times A + s \frac{\partial A}{\partial t} = 0 \quad \dots\dots (14)$$

For induction coil:

$$\nabla \times \frac{1}{m_0} \nabla \times A + s_{ind} \frac{\partial A}{\partial t} = J_s \quad \dots\dots (15)$$

Where  $\sigma_{ind}$  is the conductivity of coil material.

For air:

$$\nabla \times \nabla \times A = 0 \quad \dots\dots (16)$$

It can be shown that for the great majority of induction heating applications it is possible to further simplify the mathematical model by assuming that the currents have a steady-state quantity [5]. Thus a time-harmonic electromagnetic field can be introduced. This field can be described by the following equation [7, 8]:

$$\frac{1}{m} \nabla^2 A = -J_s + j\omega s A \quad \dots\dots (17)$$

Equation (17) is valid for general three-dimensional fields and allows one to find all of the required design

parameters of induction system such as current, power, coil impedance, and heat source density induced by eddy currents. For many induction heating applications, the quantities of the magnetic field may be assumed to be entirely directed. This allows one to reduce the three-dimensional field to a combination of two-dimensional forms. For example, in the case of magnetic vector potential, equation (17) can be expressed for an axisymmetric cylindrical system as [7]:

$$\frac{1}{m} \left( \frac{\partial^2 A}{\partial R^2} + \frac{1}{R} \frac{\partial A}{\partial R} + \frac{\partial^2 A}{\partial Z^2} - \frac{A}{R^2} \right) = -J_s + j\omega_s A \quad \dots (18)$$

The boundary of the region is selected such that the magnetic vector potential A is zero along the boundary or its gradient is negligibly small along the boundary compared to its value elsewhere in the region (Neumann condition  $\partial A / \partial n = 0$ ).

**4- Mathematical Modeling of the Thermal Processes**

In general, the transient heat transfer process in a metal workpiece can be described by Fourier equation [9]:

$$c \rho_D \frac{\partial T}{\partial t} + \nabla \cdot (-k \nabla T) = \ddot{q} \quad \dots (19)$$

Where T is the temperature,  $\rho_D$  is the density of metal, c is the specific heat, k is the thermal conductivity of

the metal, and  $\ddot{q}$  is the heat source density induced by eddy currents per unit time in a unit volume ( so-called heat generation). This heat source density is obtained by solving the electromagnetic problem. For most engineering induction heating problems, boundary conditions combine the heat losses due to convection and radiation. In this case

the boundary condition can be expressed as [9, 10]:

$$-k \frac{\partial T}{\partial n} = h_f (T_s - T_a) + C_s (T_s^4 - T_a^4) + Q_s \quad \dots (20)$$

Where  $\partial T / \partial n$  is the temperature gradient in a direction normal to the surface at the point under consideration,  $h_f$  is the convection surface heat transfer coefficient,  $C_s$  is the radiation heat loss coefficient which can be determined approximately as  $C_s = \sigma_{SB} \epsilon_s$  where  $\epsilon_s$  is the emissivity of workpiece and  $\sigma_{SB}$  is Stevan-Boltzmann constant,  $Q_s$  is the surface loss ( during cooling phase or as a result of workpiece contact with cold rolls or water-cooled guides, etc.),  $T_s$  is the surface temperature and  $T_a$  is the ambient temperature. If the heated body is geometrically symmetrical along the axis of symmetry, the Neumann boundary condition can be formulated as [11, 12]:

$$\frac{\partial T}{\partial n} = 0 \quad \dots (21)$$

The Neumann boundary condition implies that the temperature gradient in a direction normal to the axis of symmetry is zero.

In the case of heating a cylindrical workpiece, equation (19) can be rewritten as [5]:

$$c \rho_D \frac{\partial T}{\partial t} = \frac{\partial T}{\partial Z} \left( k \frac{\partial T}{\partial Z} \right) + \frac{1}{R} \frac{\partial}{\partial R} \left( k R \frac{\partial T}{\partial R} \right) + \ddot{q} \quad \dots (22)$$

Equation (22) with boundary conditions (equations (20) and (21)) are the most popular equations for mathematical modeling of the heat transfer processes in induction heating and heat treatment applications.

**5- Coupling of the Electromagnetic and Thermal Problems**

In induction heating computation, both the electromagnetic and heat transfer phenomena are tightly coupled thanks to the interrelated nature of the material properties such as [12]:

- Specific heat, thermal conductivity, and electric resistivity, which are function of temperature.
- Magnetic permeability is a function of magnetic field intensity and temperature.

There are three ways to couple the electromagnetic and heat transfer problems, and these approaches are [5, 13]:

- a. Two-steps approach: The first step is devoted to solving the electromagnetic problem. Then the obtained current densities and joule loss distribution are used as heat sources for solving the thermal problem assuming that the electrical resistivity and magnetic permeability do not change during heating. And that is a very rough postulation and can result in significant calculation error. Thus this approach can be used in a very limited number of induction heating applications.
- b. Indirect coupling approach: This method uses an iteration method which consists of an electromagnetic computation and then recalculation of heat sources in order to provide a heat transfer simulation. The temperature distribution within the workpiece obtained from the time stepped heat transfer computation is used to update the values of specific heat and thermal conductivity at each time step.

- c. Direct coupling approach: This method depends on formalizing a set of governing equations in such a way that the unknown parameters of the electromagnetic field and unknown parameters of the thermal problem will be part of one global matrix that will be solved simultaneously.

For most induction heating applications, an indirect coupling approach is valid and very effective. Therefore, this method is used in this paper.

**6- Induction Heating Representation on ANSYS**

The ANSYS computer package is a large-scale multipurpose finite element program, which may be used for solving several classes of engineering analyses. The solution of electromagnetic field computation is typically obtained by minimizing the energy function that corresponds to the governing equations (18) and (22) instead of solving that equation directly. The energy function is minimized for the integral over the total area of modeling, which includes the workpiece, coil and surrounding area. The energy function, corresponding to two-dimensional governing electromagnetic equation, can be written in the form of [5]:

$$F = \int_{vol} \left( \frac{1}{2m} \left( \left| \frac{\partial A}{\partial R} + \frac{A}{R} \right|^2 + \left| \frac{\partial A}{\partial Z} \right|^2 \right) + j \frac{WS}{2} |A|^2 - J_s A \right) d(vol) \dots (23)$$

According to FEM, the area under study is divided into nonoverlapping numerous finite

elements (mesh), therefore the minimization of the function provides minimization of energy at every node of each element. This can be arranged by setting the first partial derivative of the function with respect to each node, equal to zero. After some algebraic operations, the local matrix equation which represents the minimization of the energy function within any element and then the total (global) energy associated with the whole area of modeling can be obtained. As a result, a set of simultaneous equations with respect to the unknown values of magnetic vector potential at each element  $[A_e]$  can be written as [13]:

$$[C^{AA}] \frac{d}{dt} [A_e] + [K^{AA}] [A_e] = [J^S] \dots (24)$$

Where  $[C^{AA}]$  = Magnetic damping matrix,  $[K^{AA}]$  = Vector magnetic potential coefficient matrix,  $[J^S]$  = Applied load (current density).

By solving the system of equations and obtaining the magnetic vector potential  $[A_e]$  through the model it is possible to find all of the required parameters as follows:

(a) – Magnetic flux density  $[B]$ :

$$[B] = \nabla \times [N_A]^T [A_e] \dots (25)$$

Where  $[N_A]$  is a matrix of element shape functions.

(b) – Magnetic field intensity  $[H]$ :

$$[H] = [n] [B] \dots (26)$$

Where  $[n]$  is the reluctivity matrix,  $[v] = [\mu]^{-1}$

(c) – Eddy current density  $J_e$ :

$$J_e = -[S] \left\{ \frac{\partial A}{\partial t} \right\} = -[S] \frac{1}{m} \sum_{i=1}^m [N_A]^T \{dA_{ei}\} \dots (27)$$

m is the number of integration points (i) and  $\{dA_{ei}\}$  is the time derivative of magnetic vector potential.

(d) – Joule heat HGEN:

$$HGEN = Re \left( \frac{1}{2m} \sum_{i=1}^m [r] [J_{ei}] [J_{ei}]^* \right) \dots (28)$$

Where  $[J_{ei}]$  is the complex eddy current density in the element at integration points,  $[\rho]$  is the resistivity matrix.

By following the same procedure, used to obtain the FEM modeling of electromagnetic side of induction heating (eq.2.24), the following equation can be written to represent the thermal process of induction heating [13]:

$$[C_e^t] \{T_e\} + ([K_e^{tb}] + [K_e^{tc}]) \{T_e\} = \{Q_e^c\} + \{Q_e^s\} \dots (29)$$

Where  $\{T_e\}$  is the nodal temperature vector of element,  $[C_e^t]$  = Element specific heat (thermal damping matrix),  $[K_e^{tb}]$  = Element diffusion conductivity matrix,  $[K_e^{tc}]$  = Element convection surface conductivity matrix,  $\{Q_e^c\}$  = Element convection



surface heat flow vector,  $\{Q_e^s\}$  = Element heat generation load. Equation (29) includes heat transfer and convection losses. To evaluate radiation loss, the following equation is used [13]:

$$Q_{rad} = k'(T_s + 273) - (T_a + 273) \quad \dots(30)$$

Where  $K'$  is a function of the unknowns surface temperature ( $T_s$ ) and ambient temperature ( $T_a$ ). Temperatures from previous iteration of equation (29) are used to calculate  $K'$ , and the solution is computed iteratively to determine the temperature distribution through the workpiece  $\{T_e\}$ , also the thermal losses developed during the heating period.

## 7- Building an Induction Heating Model

In ANSYS environment, most of tasks can be performed either by Graphical User Interface (GUI) or by ANSYS Parametric Design Language (APDL). In this work, APDL is used because it encompasses a wide range of features, such as repeating, branching, macros, etc. Figure (1) shows a sample of induction heating systems which are studied in this work. Figure (2) shows a cross section of that furnace. The required dimensions to specify any induction heating system are: vertical length of charge ( $L_w$ ), radius of charge ( $r_w$ ), coil inner diameter ( $r_{ic}$ ), coil length ( $L_c$ ) (normally equals to charge length), number of turns per one layer of induction coil ( $tpl$ ), radial thickness of conductor ( $th$ ), and axial space factor of coil ( $K_a$ ). For

multilayer coil, all the previous items are required, in addition to, number of layers ( $N$ ) and radial space factor of the coil ( $K_r$ ). The width of coil conductor ( $h$ ) can be evaluated as:

$$h = \frac{L_c}{1 + \frac{tpl-1}{K_a}} \quad \dots\dots (31)$$

### 7.1- The Electromagnetic Model

The model of induction furnace should be surrounded by a boundary region, because it is unbounded problem, so a boundary volume of the hollow sphere is used, the outer radius of sphere is about twice the largest dimension of the model.

From figure (2), it is clear that the model is of rotational symmetry, so it is reduced to axisymmetric model. An axisymmetric model of single layer induction furnace is shown in figure (3). For two-dimensions, axisymmetric and electromagnetic analysis, a PLANE53 element is used, this element is 8-node quadrilateral shape and it is used to discretize the workpiece, the coil and the air regions. For the boundary region, an INFIN110 element is used; it is quadrilateral 8-node element. In order to mesh the model, the following points have to be taken into account [5, 14]:

- 1- If the mesh is too coarse, the results can contain a serious error.
- 2- If the mesh is too fine, the model may be too large to run on the computer or it takes a long run time.

In order to combine accuracy and quickness in meshing the model, the mesh is made as dense as possible in the sensitive zones (near the outer surface of the workpiece and near the

induction coil) and less mesh density is used near the centerline of the workpiece and near the boundary region. Figure (4) shows the meshed induction heating model.

### 7.2- The Thermal Model

Most of induction heating applications consist of a water cooled induction coil to maintain the coil operating temperature within an acceptable level during the heating cycle. A notable increase in temperature appears inside the workpiece only. So, the thermal model includes just the workpiece. PLANE55 element is used to discretize the workpiece region; this element is 4-node with a 2-dimension thermal conduction capability. Meshing of the workpiece has same density as in electromagnetic model, because the rise of temperature is faster and higher near the outer surface than at centerline.

### 7.3- Defining Material Properties and Boundary Conditions

One of the most important advantages of ANSYS is the ability to take the temperature-dependant material properties into account. For non-magnetic workpiece, temperature dependant material properties include: resistivity, thermal conductivity, and specific heat.

For the electromagnetic field, INFIN110 element is used to model an open boundary of unbounded field problem where a number of this element forms a boundary layer surrounding the model; the exterior surface of the layer represents the infinite surface.

A flux-parallel boundary condition is specified at the centerline of the model, this

boundary condition ensures that the flux does not leak out of the model due to the axisymmetry.

For the thermal field, uniform initial temperature of 25°C is applied to the workpiece and constant ambient temperature of 25 °C is specified.

### 7.4- Multifield Solver

In induction heating problems, the electromagnetic model (field) calculates joule heat generated inside workpiece, which is used in transient thermal analysis to predict a time-dependent temperature solution. When the input of one field depends on the results of another field, the fields are coupled. Coupling of electromagnetic and thermal fields can be accomplished by either matrix coupling (direct coupling) or sequentially coupling (indirect coupling). ANSYS 8.0 introduces a new solver available for a large class of coupling problem. This solver is called multifield solver.

Multifield solver is an automated tool for solving sequentially coupling field problems. Algorithm of multifield solver, as shown in figure (5), consists of three loops: field loop, stagger loop and time loop. The time loop corresponds to the time step loop of the multifield problem, the time step represents the actual end time and time step. Within each time loop is the stagger loop, the stagger loop allows for implicit inter-relationship between the fields in the multifield solution within each step in the time loop, the field solutions are repeated in the stagger loop until convergence. Within each stagger loop is the field loop, which contains the analysis of each field solution. The field loop is setup like any single ANSYS analysis.



### 7.5- Analysis of Induction Furnaces by APDL Program

The procedure of solving an induction heating model by multifield solver is started by solving the electromagnetic field and evaluating the Degree Of Freedom (DOF). DOF for electromagnetic field is magnetic vector potential. Depending on the distribution of the magnetic vector potential through the workpiece, Joule heat per unit volume (HGEN) can be calculated (equations 27 and 28).

Multifield solver automatically transfers HGEN from the electromagnetic to the thermal field. The thermal model, according to the values of HGEN, determines the DOF which is the temperature distribution through the workpiece. Multifield solver transfers temperature to the electromagnetic field and updates the values of temperature-dependant properties.

Timing of the multifield solver is specified as follow:

- End time for a multifield solution is set to 240 second for all simulated cases in this work.
- Time step increment for a multifield is set to 5 second.
- Time step increment for each field is specified to a range of (0.05-0.1) second.

With reference to the steps of building an induction heating model and by using multifield solver, a main program is prepared. This program has a great flexibility to deal with cylindrical induction heating systems of any dimensions, and it can be used to simulate single layer or multilayer furnaces of non-magnetic workpiece and for various power supply conditions. The induction heating model analyzed in this study

is similar to a practical model of reference [4], the dimensions of this model are listed in table (1). A series of different cases were studied and those cases can be summarized as:

- a- Single-layer induction heater: Models were carried out for different supplied frequencies within a range of (1-40) kHz.
- b- Multi-layer induction heater: Models were carried out for different number of layers within a range of (5-40) layers.

### 7.6- Review the Results of the APDL Program

Results can be viewed as figures or tables by using the following postprocessors:

- a- The general postprocessor reviews analysis results over the entire model or selected portions of the model at a single time.
- b- The time-history postprocessor reviews analysis results at specific locations in the model as a function of time.

The time required, to analyze an induction furnace, depends on: the complexity of the model, the period of heating cycle, and the time step increment for field analysis. For example, single layer induction furnace supplied by  $15\text{A/mm}^2$  (1409A), 10 kHz, heating cycle time is 240 second and time step increment for field analysis is within a range of (0.05-0.1) second, analysis of this furnace took about 36 minutes. The results obtained from analyzing this furnace are shown in the following figures, where figure (6) shows 2-dimensions distribution of the magnetic flux lines. Figure (7) shows a vector representation of magnetic flux density inside the workpiece. Due to the induction

principle, an eddy current is induced inside the workpiece; the vector representation of the eddy current density inside the workpiece is shown in figure (8). The eddy current produces heat by the joule effect. Figure (9) shows the distribution of the power dissipated as heat inside the workpiece per unit volume. The distribution of temperature through the workpiece at the end of the heat cycle is shown in figure (10), while figure (11) shows the rise of temperatures during the heating cycle at specific points inside the workpiece.

#### 7.7- Efficiency and Power Factor of the Induction Furnace

In addition to the results given above, it is important to evaluate the efficiency and the power factor of the induction furnace. Depending on a set of equations suggested by Harvey [5], and using the facilities of ANSYS package, a general program is designed to calculate the efficiency and the power factor for any induction heating system (single or multi layer). The results of the program are compared with published practical measurements of multilayer induction heater obtained by Abood [15]. A good agreement between the practical values and those calculated by the program is clear in tables (2) and (3).

Due to presence of practical measurements of efficiency and power factor of an induction furnace, so it has been satisfied with those measurements to appraise the suitability and the accuracy of the analysis used in this work

#### 7.8- Induction Heating System with Magnetic Workpiece

For workpiece of magnetic material, the magnetic permeability is a complex function of magnetic field intensity and temperature, which has a marked effect on the behavior of the induction heating. In ANSYS, magnetic permeability can be defined as a temperature-dependant material property, but the effect of changing the magnetic field intensity is ignored here. For applications of small change in temperature, it can be assumed that the temperature is constant and the permeability values are specified by defining the B-H curve at that temperature. Most of induction heating applications involve a tremendous increase in temperature inside the workpiece, which compel to make a constant temperature assumption that is impractical. In ANSYS environment the magnetic permeability cannot be defined as a function of both magnetic field intensity and temperature. To overcome this problem, the multiregion method is suggested. The application of multiregion method includes the following steps:

- a. Dividing the workpiece longitudinally into multiregions.
- b. Estimating the values of magnetic field intensity for each region.
- c. By considering that the magnetic field intensity is constant for each region, curves of magnetic permeability as a function of temperature for each region can be obtained.
- d. Now, by specifying the magnetic permeability for all regions, the system can be solved normally as described early.

To verify the applicability and the accuracy of the multiregion method for analyzing an induction heating system with magnetic workpiece, this method is applied to an induction furnace described and analyzed by Barglik [16], by using FEM-based package called QuickField. According to multiregion method, the workpiece is divided into two regions as shown in figure (12). Figure (13) shows the temperature-time response of two different points inside the workpiece as compared with the results of reference [16].

### 8- Conclusions

Induction heating systems have been widely accepted to possess number of inherent advantages and benefit over other heating systems in industrial applications. It is to be noted that big efforts are made to develop the induction heating depending on the modern advances in the computational approaches. The following are the conclusions derived from the present work:

- 1- Nowadays, the perfect approach to analyze the induction heating system is the use of one of the specialized computer packages which are based on one of numerical methods. The good agreement between the practical measurements and the results obtained in this work appears that ANSYS is a robust tool to analyze the induction furnaces and that the procedure of analysis is valid and the programs which are used accurate.
- 2- Limitations of ANSYS, when dealing with magnetic material properties, especially permeability where it treated as a function of only one variable

while in fact it is function of both temperature and magnetic field strength. To overcome such deficiency in ANSYS, a multiregion method is proposed yielding good results for induction furnaces with magnetic workpiece.

### References

- [1] Davies, J. and Simpson, P., "Induction Heating Handbook", McGraw-Hill book Company (UK), 1979.
- [2] Martin, D.H., "High Efficiency Induction Billet Heater", 10<sup>th</sup> Congress of Electroheat, Stockholm, 1984.
- [3] Harvey, I.G. and Martin, D.H., "Energy Conservation and the Multilayer Coil Induction Heater", IEE Colloquium On Electroheat Processing Of Materials Using Electricity, 1981.
- [4] Harvey, I.G., "The Theory of Multi-Layered Winding for Induction Heating and Their Application to 1MW, 50 Hz, Longitudinal Flux Billet Heater", ECRC/R992, 1976.
- [5] Rudnev, R., Loveless, D., Cook, R. and Black, M., "Handbook of Induction Heating", MARCEL DEKKER Inc., New York, 2003.
- [6] Hayt, W.H. and Buck J.A., "Engineering Electromagnetics", 6<sup>th</sup> edition, McGraw-Hill, 2001.
- [7] Matthew, N.Sadiku, "Numerical Techniques in Electromagnetic", 2<sup>nd</sup> edition, CRC Press, USA, 2001.
- [8] Kurek, K., "Optimization of Induction Heater Construction", International Seminar on: Simulation and Identification of Electroheat Processes-University of Lodz, June 1997.
- [9] Landek, D., Cajner, F. and Filetin, T., "Computer Simulation of Induction Surface Hardening Axially Symmetric Workpieces", Journal de

Physique, Vol. -120, pp. 499, Dec. 2004.

[10] Barglik, J. and Skopek, M., "Mathematical and computer modeling of induction hardening", Acta Technica CSAV-46, pp. 227-250, 2001.

[11] Valirntin, S., Vladimir, A. and Dmitri, V., "Computer Simulation of Induction Heating and Quenching Processes", Centre for Induction Technology, 1999.

[12] Klimpke, B. and Rebizant, C., "Two and Three Dimensional Coupled Electromagnetic/Thermal Analysis for Induction Heating Application Using the Boundary Element Method (BEM)", Integrated Engineering Software, 1997.

[13] ANSYS Release 11.0, Documentation, 2007.

[14] FLUX2D application- Induction Heating Tutorial- CEDRAT, Dec. 2003.

[15] Al-Shaikhli, A.K.M., Alwash, S. and Abood, M., "Method of Analysis for Multilayer Induction Heating Coils", Mag. of Engineering and Technology, university of Technology, Vol-11, pp. 26-41, 1992.

[16] Barglik, J., Dolezel, K., Ducki, K. and Ulrych, B., "Induction Heating and Consequent Hardening of a Ferromagnetic Cylinder in Various Cooling Media", Materially XXIV Miedzynarodowej Konferencj IC-SPETO 2001.

**Table (1) The dimensions of the induction heating model**

$L_c=L_w$	0.5 m
row	0.05 m
ric	0.075 m
tpl	30
th	0.007 m
$K_a$	0.8
$K_r$	0.8

**Table (2) Comparison between the calculated and measured efficiency**

Number of layers	Efficiency (%)		Error (%)
	Experimental	Calculated	
1	15.54	15.19	2.25
2	27.81	25.86	7
3	35.51	33.69	5.1
4	42.18	39.65	5.9

**Table (3) Comparison between the calculated and measured power factor**

Number of layers	Power factor		Error (%)
	Experimental	Calculated	
1	0.535	0.522	2.3
2	0.33	0.32	2.3
3	0.267	0.261	2.1
4	0.239	0.233	2.3

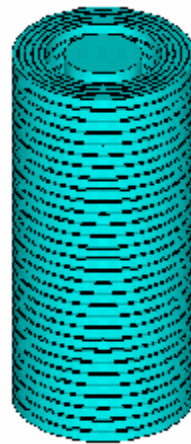


Figure (1) Schematic diagram of a multilayer induction heating system

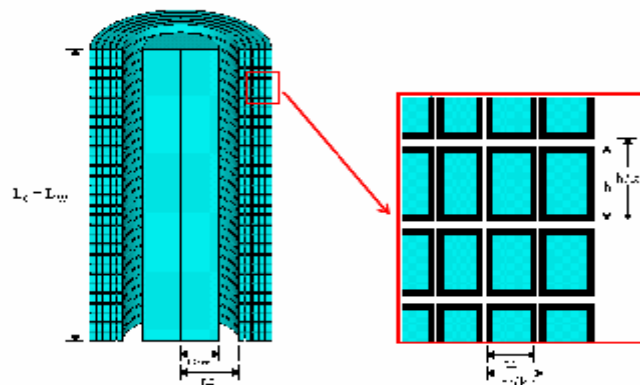


Figure (2) A cross section of multilayer induction heater

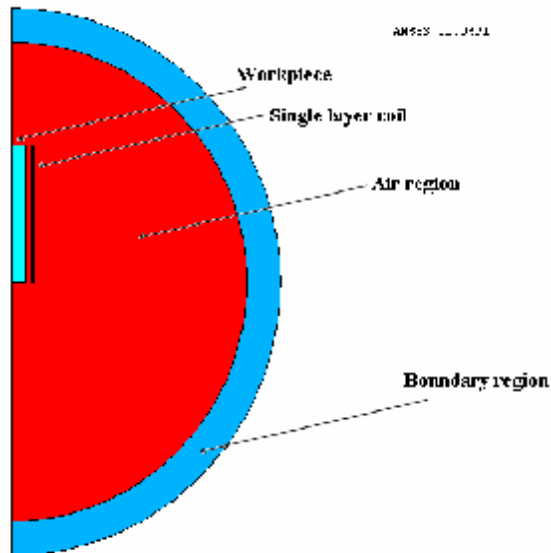


Figure (3) A cross section of single layer furnace with the boundary region

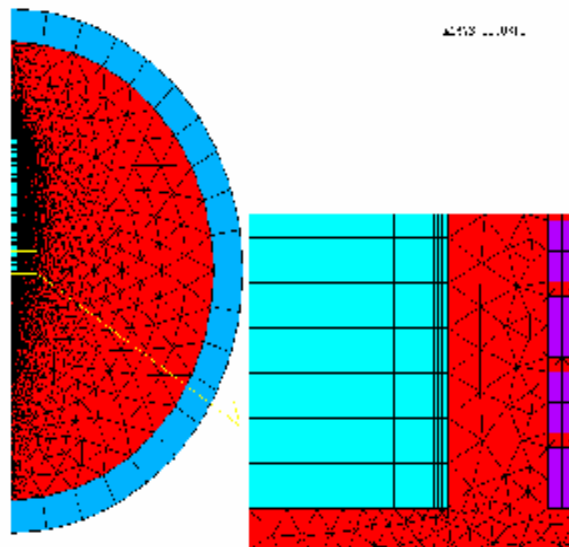


Figure (4) Meshed model of induction heating furnace



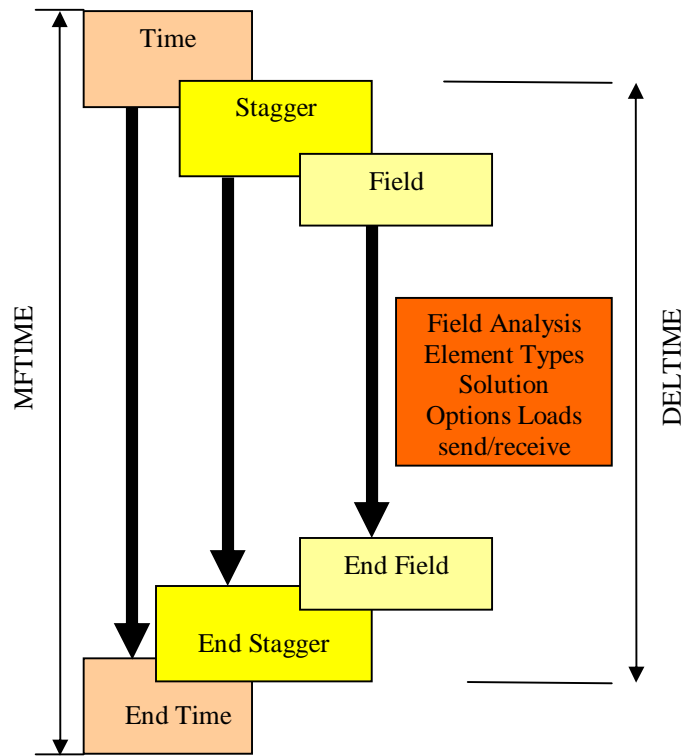


Figure (5) The algorithm of multifield solver

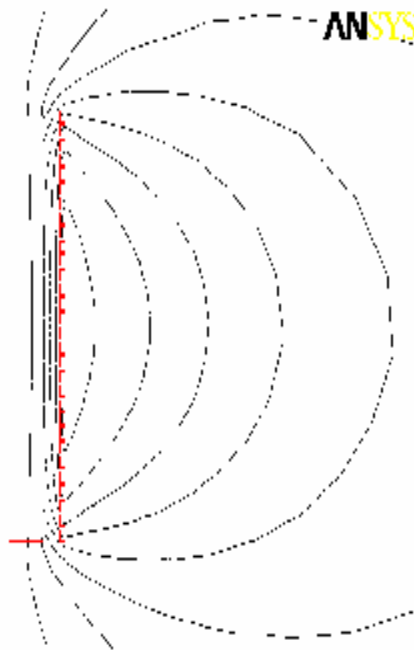


Figure (6) Distribution of the magnetic flux lines

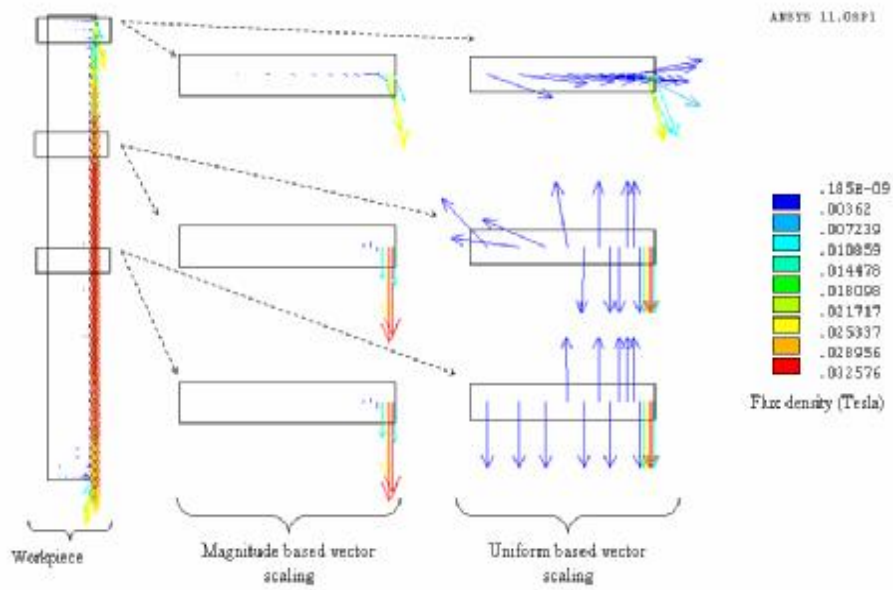


Figure (7) The magnetic flux density inside the workpiece

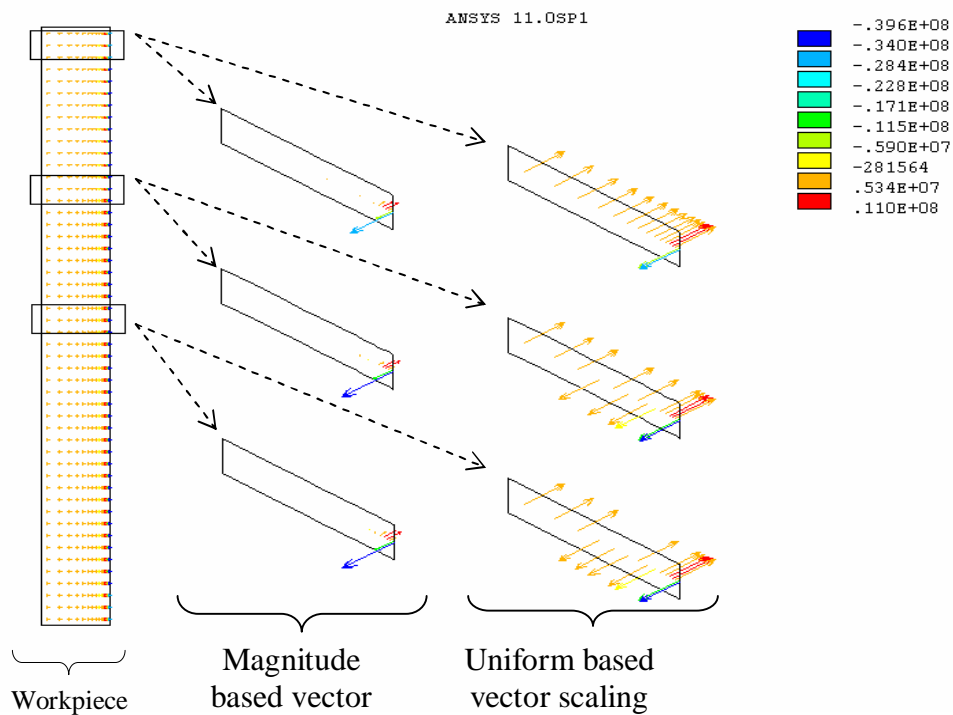


Figure (8) Eddy current density inside the workpiece

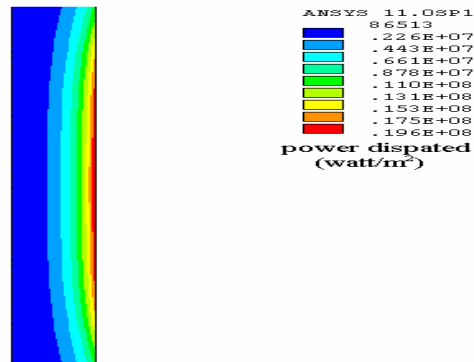


Figure (9) Distribution of the power dissipated per unit volume inside the workpiece

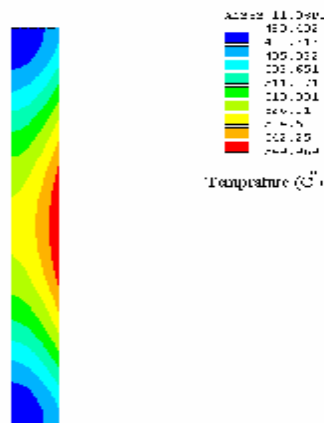


Figure (10) Heat distribution at the end of heating cycle

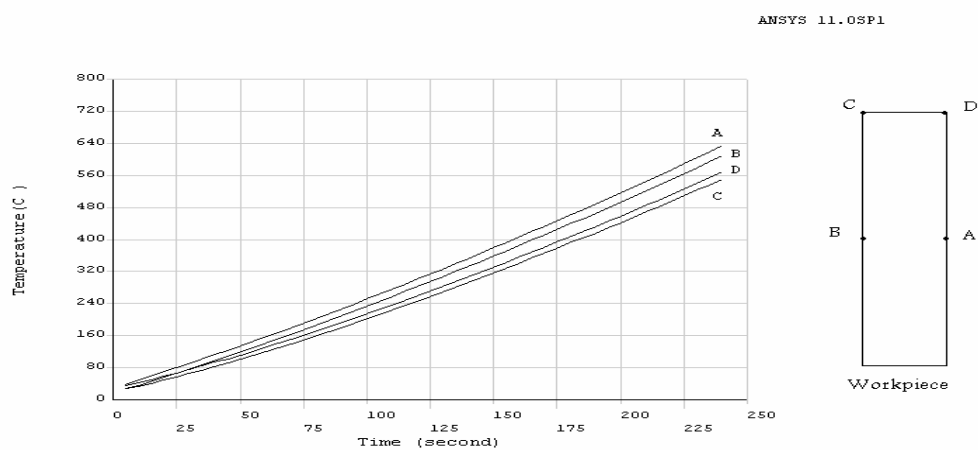


Figure (11) The rise of the temperatures at specific points inside the workpiece

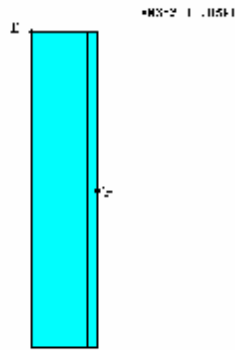


Figure (12) Longitudinal section of the workpiece divided into two regions

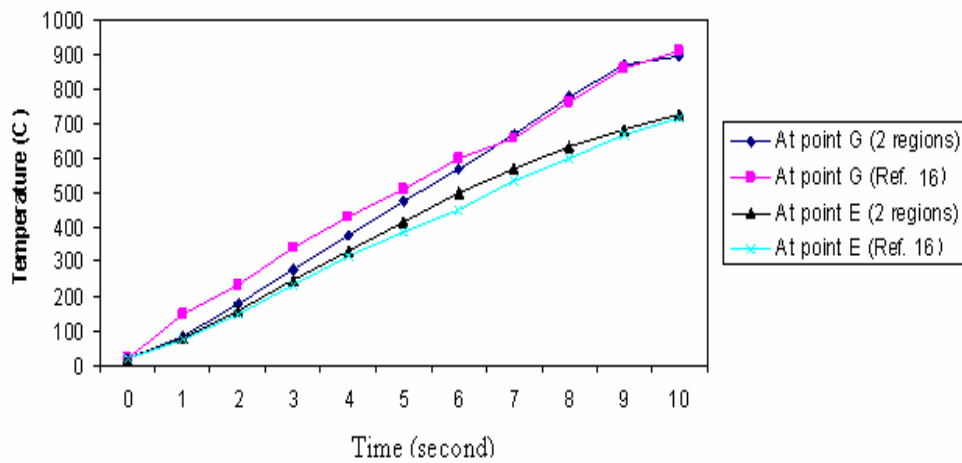


Figure (13) Temperature rise at two different points